Synthesis, Biological Evaluation, and Receptor Docking Simulations of 2-[(Acylamino)ethyl]-1,4-benzodiazepines as κ-Opioid Receptor Agonists Endowed with Antinociceptive and Antiamnesic Activity

Maurizio Anzini,*[,†] Laura Canullo,[†] Carlo Braile,[†] Andrea Cappelli,[†] Andrea Gallelli,[†] Salvatore Vomero,[†] M. Cristina Menziani,[‡] Pier G. De Benedetti,[‡] Milena Rizzo,[§] Simona Collina,[||] Ornella Azzolina,[||] Massimo Sbacchi,[$,#] Carla Ghelardini,[^] and Nicoletta Galeotti[^]

Dipartimento Farmaco Chimico Tecnologico, Università degli Studi di Siena, Via A. Moro, 53100 Siena, Italy; Dipartimento di Chimica, Università degli Studi di Modena e Reggio Emilia, Via Campi 183, 41100 Modena, Italy; Dipartimento di Scienze Farmacobiologiche, Università degli Studi "Magna Græcia" di Catanzaro, Complesso "Ninì Barbieri", 88021 Roccelletta di Borgia (CZ), Italy; Dipartimento di Chimica Farmaceutica, Università degli Studi di Pavia, Via Taramelli 12, 27100 Pavia, Italy; GlaxoSmithKline, Via Zambeletti, Baranzate di Bollate, 20021 Milano, Italy; Dipartimento di Farmacologia Preclinica e Clinica "M. Aiazzi Mancini", Università degli Studi di Firenze, Viale G. Pieraccini 6, 50139 Firenze, Italy

Received January 13, 2003

The synthesis and biological evaluation of a series of new derivatives of 2-substituted 5-phenyl-1,4-benzodiazepines, structurally related to tifluadom (**5**), are reported. Chemical and pharmacological studies on compounds **6** have been pursued with the aim of expanding the SAR data and validating the previously proposed model of interaction of this class of compounds with the κ-opioid receptor. The synthesis of the previously described compounds **6** has been reinvestigated in order to obtain a more direct synthetic procedure. To study the relationship between the stereochemistry and the receptor binding affinity, compounds **6e** and **6k** were selected on the basis of their evident structural resemblance to tifluadom. Since a different specificity of action could be expected for the enantiomers of **6e** and **6k**, owing to the results shown by (*S*)- and (*R*)-tifluadom, their racemic mixtures have been resolved by means of liquid chromatography with chiral stationary phases (CSP), and the absolute configuration of the enantiomers has been studied by circular dichroism (CD) and ^{1}H NMR techniques. Moreover, some new 2-[(acylamino)ethyl]-1,4-benzodiazepine derivatives, **6a**−**d**,**f**,**g**,**j**, have been synthesized, while the whole series (**6a**−**o**) has been tested for its potential affinity toward human cloned κ-opioid receptor. The most impressive result obtained from the binding studies lies in the fact that this series of 2-[2-(acylamino)ethyl]-1,4-benzodiazepine derivatives binds the human cloned κ-opioid receptor subtype very tightly. Indeed, almost all the ligands within this class show subnanomolar K_i values, and the least potent compound **6o** shows, in any case, an affinity in the nanomolar range. A comparison of the affinities obtained in human cloned κ-receptor with the correspondent one obtained in native guinea pig κ-receptor suggests that the human cloned κ-receptor is less effective in discriminating the substitution pattern than the native guinea pig κ-receptor. Furthermore, the results obtained are discussed with respect to the interaction with the homology model of the human κ-opioid receptor, built on the recently solved crystal structure of rhodopsin. Finally, the potential antinociceptive and antiamnesic properties of compounds **6e** and **6i** have been investigated by means of the hot-plate and passive avoidance test in mice, respectively.

Introduction

Opioids have attracted increasing interest, primarily because of their powerful pain-relieving properties and their potential tendency toward addiction. Opioids exert their actions through four types of receptors, μ, δ, κ,[1] and ε,[2] belonging to the G-protein coupled receptor (GPCR) superfamily of integral proteins. Although it is now well established that three of them (i.e. μ-, δ-, and κ-receptors) are present in the central and peripheral nervous system of many species, including man, the existence of the ε-opioid receptor has been controversial and only recently has a paper appeared supporting evidence for ε-opioid receptor mediated β-endorphin-induced antinociception in some animal models.[2] A precise classification of opioid receptors followed the discovery of their specific endogenous neuropeptides: Met^5- and Leu^5-enkephalins for the μ- and δ-sites and dynorphins for κ-sites.[3]

Thus, research into the mechanism of opioid actions has focused on the function of each opioid receptor type and on the functional interaction between the individual receptor types. Development of selective receptor ligands and, particularly, recent cloning of receptors have provided efficient tools for the study of the function of these receptors.[4] A considerable interest has developed

* To whom correspondence should be addressed. Tel.: +39 0577 234 173. Fax: +39 0577 234 333. E-mail: anzini@unisi.it.
† Università degli Studi di Siena.
‡ Università degli Studi di Modena e Reggio Emilia.
§ Università degli Studi "Magna Græcia" di Catanzaro.
|| Università degli Studi di Pavia.
$ GlaxoSmithKline.
# Present address: Via G. Rossa, 20090 Assago, Milano.
^ Università degli Studi di Firenze.

10.1021/jm0307640 CCC: $25.00
Published on Web 08/06/2003

Chart 1

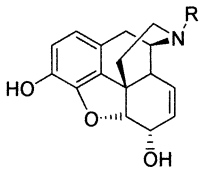

1a, R = methyl, morphine
1b, R = allyl, nalorphine

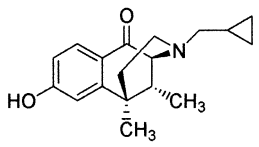

2, ketocyclazocine

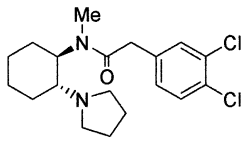

(±)-**3**, U-50488

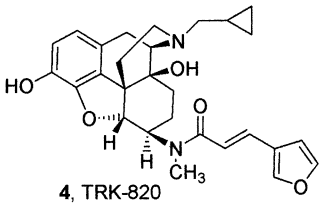

4, TRK-820

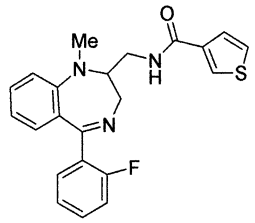

5, tifluadom

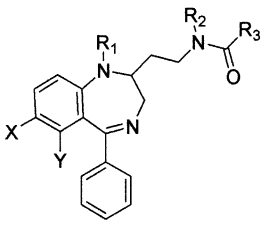

6

during the past decade around the research of selective, nonpeptidic, κ-opioid receptor agonists as safe and effective antinociceptive agents. In particular, these compounds are able to keep the antinociceptive potency of morphine (**1a**) (the prototype agonist at the μ-receptor) in the absence of the typical side effects of morphine-like drugs: gastrointestinal constipation, respiratory depression, physical dependence liability, and high addiction potential.[5]

Administration of κ-opioid receptor agonists, however, is also associated with a spectrum of side effects including diuresis, sedation/locomotor incoordination, and an array of central nervous system (CNS) effects.[5]

Interestingly, many studies suggest that the activation of the κ-receptor suppresses the antinociceptive effect of μ-receptor agonists. In fact, systemic (intracerebroventricular or intraperitoneal) administration of dynorphin or U-50488 (**3**) dose-dependently antagonizes the antinociception induced by morphine, a weakly selective μ-receptor agonist[6,7] in tail-flick and hot-plate tests in mice, rats, or guinea pigs.[8] The anti-μ-receptor-mediated action of κ-receptors has also been reported in learning and memory processes in the brain. In behavioral studies, the selective activation of the μ-receptor by Tyr-DAla-Gly-[*N*MePhe]-NH$(CH_2)_2$–OH (DAMGO) impairs working memory-associated spontaneous alternation performance in mice, but dynorphin, at otherwise ineffective doses on the control performance, significantly improves the DAMGO-induced memory impairment.[9] The first two non-peptide κ-agonist antinociceptives, though they have a limited selectivity for the κ-receptor, were nalorphine (**1b**), the N-allyl derivative of morphine, and ketocyclazocine (**2**), a benzomorphan derivative (Chart 1) lacking some of the typical effects of morphine.[10] The research was also enhanced by the discovery[11] that simple *trans*-diaminocyclohexane derivatives, such as U-50488 (**3**), display a very high selectivity for κ-opioid receptors along with a side-effect profile more evident than benzomorphan.[12] Furthermore, Toray Industries Inc. focused their efforts on the discovery and development of TRK-820 (**4**), an *N*-cyclopropylmethylmorphine derivative, an atypical, potent κ-opioid agonist with a μ-partial agonist profile as well as a weak ORL-1 antagonist component. This compound entered phase II clinical trials for pain treatment in both Japan and the US in 1997.[13] In two recent patent applications filed by Toray, TRK-820 and related morphinan κ-agonists are claimed to be of particular efficacy in the treatment of neuropathic pain[14] and as cornea and conjunctiva antipruritics.[15] TRK-820 also appears to be a promising potential drug among opiates, particularly for the apparent lack of centrally related side effects at therapeutic doses. Selective affinity for κ-receptors has also been identified in different structures, such as the 1,4-benzodiazepine derivative tifluadom (**5**),[16] which, however, was found to interact also with CCK-A receptors.[17] In a previous paper, we described the synthesis and biological evaluation of a series of 2-substituted 5-phenyl-1,4-benzodiazepines **6**, structurally related to tifluadom (**5**), which bound with nanomolar affinity and high selectivity to κ-opioid receptors with respect to both opioid μ- and δ-subtypes and to CCK-A receptors. In particular, the 2-thienyl derivative **6e** with a $K_i = 0.50$ nM represented a clear improvement with respect to tifluadom, showing a comparable potency but higher selectivity. Furthermore, the application of computational simulations and linear regression analysis techniques to the complexes of guinea pig $\kappa(\kappa_1)$ receptor and the synthesized compounds allowed the identification of the structural determinants for the recognition and quantitative elucidation of the structure−affinity relationships in this class of receptors.[18]

Besides, some important clues on the structural elements that confer high affinity/selectivity were derived. On the basis of these results, chemical and pharmacological studies on compounds **6** have been pursued with the aim of expanding the SAR data and of validating the model proposed. The synthesis of the previously described compounds **6** has been reinvestigated in order to obtain a more direct procedure.

Since a different specificity of action could be expected for the enantiomers of **6e** and **6k**, owing to the results shown by (*S*)- and (*R*)-tifluadom,[19−22] their racemic mixtures have been resolved by means of liquid chromatography with chiral stationary phases (CSP), and the absolute configuration of the enantiomers has been studied by circular dichroism (CD) and ^{1}H NMR techniques.[23]

Moreover, some new 2-[(acylamino)ethyl]-1,4-benzodiazepine derivatives, **6a**−**d**,**f**,**g**,**j**, have been synthesized, while the whole series (**6a**−**o**) has been tested for potential affinity toward human cloned κ-opioid receptor. The results obtained are discussed with respect to the interaction with the homology model of the human κ-opioid receptor built on the recently solved crystal structure of rhodopsin.[24]

Finally,the potential antinociceptive and antiamnesic properties of compounds **6e** and **6i** have been investi-

Scheme 1[a]

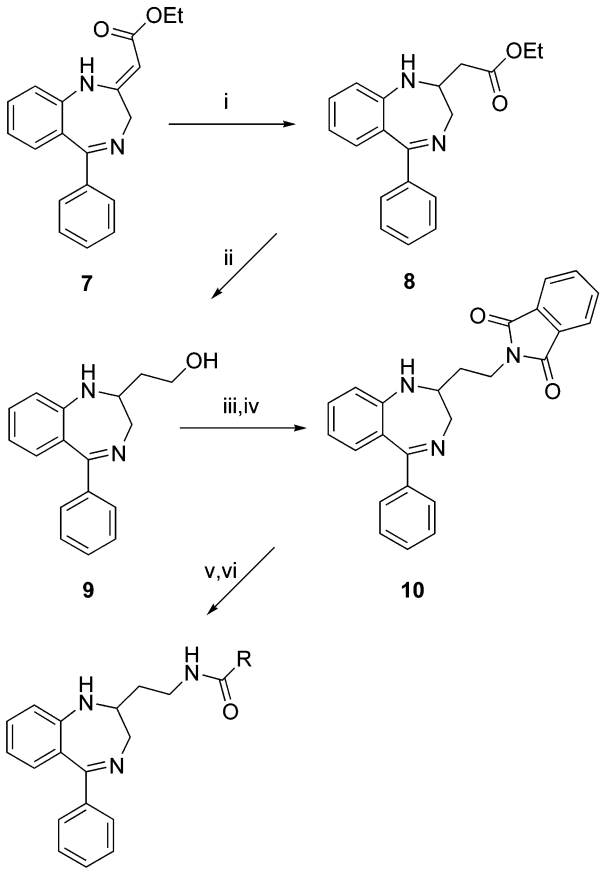

[a] Reagents: (i) Et_3SiH, TFA; (ii) $LiAlH_4$, Et_2O; (iii) $SOCl_2$, CH_2Cl_2; (iv) potassium phthalimide, NaI, DMF; (v) NH_2NH_2, MeOH; (vi) R-COCl, Et_3N, THF.

gated by means of the hot-plate and passive avoidance test in mice, respectively.[25]

Chemistry. Our efforts toward synthesis began with the application of the previously described procedure[18] for the preparation of nor-derivatives **6a**−**d** from key intermediate **7** (Scheme 1). Selective reduction of **7** with triethylsilane in trifluoroacetic acid yielded the saturated ester **8**, which was reduced with lithium aluminum hydride to afford the expected 2-(2-hydroxyethyl)-1,4-benzodiazepine **9**. This compound was transformed into target nor-derivatives **6a**−**d** in four steps via phthalimido derivative **10**.

Since the previously described synthesis of key intermediate **7** concerned a complex multistep sequence,[26,27] we realized that the preparation of this class of κ-opioid ligands **6** could be significantly improved through the development of a more direct procedure from commercially available 2-aminobenzophenone (**11a**) to key intermediate **7**. The initial attempts at direct synthesis of **7** concerned the reaction of either *tert*-butyl acetate or ethyl acetate carbanions with the iminophosphonate generated in situ from benzodiazepinone **12a** and diethyl chlorophosphate in the presence of sodium hydride. Unfortunately, such an attractive procedure did not give synthetically useful yields. On the other hand, the reaction of benzodiazepinone **12a** with the phosphoryl-stabilized anion of dimethyl malonate[28] gave good yields of diester **13a** (Scheme 2), which underwent

Scheme 2[a]

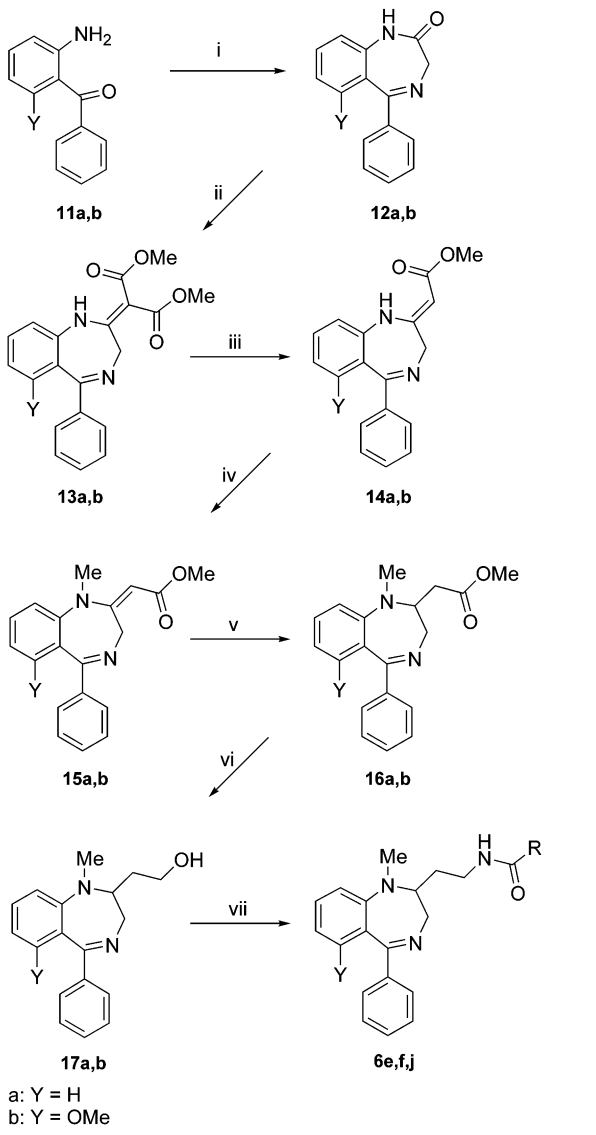

[a] Reagents: (i) NH_2CH_2 COOEt, pyridine; (ii) $CH_2(COOMe)_2$, NaH, $ClPO(OEt)_2$, DME; (iii) 3 N NaOH, MeOH; (iv) $(Bu)_4N^+Br^-$, $TsOCH_3$, 50% NaOH, benzene; (v) Et_3SiH, TFA; (vi) $LiAlH_4$, THF; (vii) (a) $SOCl_2$, CH_2Cl_2; (b) potassium phthalimide, NaI, DMF; (c) NH_2NH_2, MeOH; (d) ClCOR, Et_3N, THF.

partial hydrolysis and spontaneous decarboxylation to afford the ylidene acetic ester **14a**.[29] This compound was *N*-methylated with methyl *p*-toluenesulfonate in a two-phase system in the presence of tetrabutylammonium bromide as a phase-transfer catalyst to give *N*-methyl derivative **15a**. A two-step reduction of **15a** led to the expected 2-(hydroxyethyl)-1,4-benzodiazepine **17a**, which was transformed into target derivative **6e** in four steps following the chemistry already described. This procedure allowed an easier synthesis of substantial amounts of previously described **6e** (for the enantiomeric resolution and an extensive pharmacological testing of **6e**) and of its new derivatives **6f**,**j**. Tertiary amide derivative **6g** was obtained by *N*-methylation of **6e** with methyl iodide in the presence of sodium hydride (Scheme 3).

Among the newly designed compounds, iodo derivatives **6p**,**q** (Scheme 4) and the synthetically related acetyl derivatives **6r**,**s** could not be synthesized by means of the above-described procedure. In fact, when

Scheme 3[a]

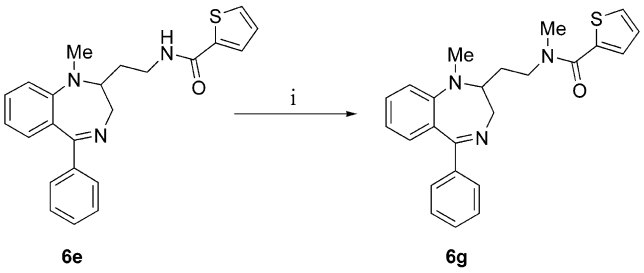

[a]Reagents: (i) MeI, NaH, DMF.

Scheme 4[a]

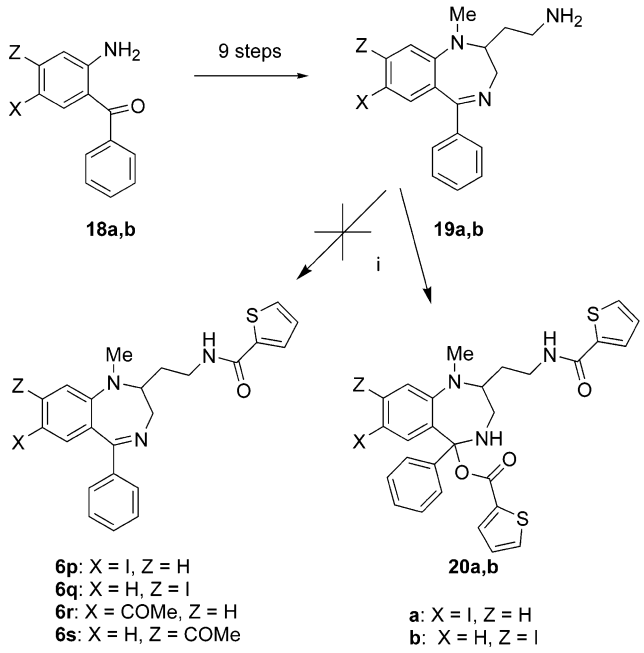

[a] Reagents: (i) 2-thienyl-COCl, Et_3N, THF.

the iodoamines **19a**,**b** were acylated with 2-thiophenecarbonyl chloride under the usual conditions, the formation of compounds **20a**,**b** was observed. These compounds appear to derive from the normal attack of the amino group by the 2-thiophenecarbonyl chloride and the addition of 2-thiophenecarboxylic acid to the imino double bond. Although we have no reasonable explanation for this result, we believe that the aromatic iodine atom could play a peculiar role.

Resolution of Racemic 6e and 6k and Configurational Analysis. To investigate the relationship between stereochemistry and receptor binding affinity, compounds **6e** and **6k** were selected on the basis of their clear structural resemblance with tifluadom. Thus, a direct HPLC method of enantiomeric separation was applied to the resolution of racemates, and the scaling up of the process was performed to obtain the pure enantiomers for the biological investigation of their enantioselectivity.

Baseline separation of both racemates was obtained by the analytical columns (250 × 4.6 mm, 5 μm) Chiralcel OJ-R and Chiralpak AD (Daicel Chemical Industries). Therefore, the semipreparative column Chiralpak AD (250 × 20 mm, 10 μm) was used to separate suitable amounts of the pure enantiomers. The enantiomeric excess of optical antipodes was calculated on the corresponding chromatographic peaks of the analytical monitoring. Very high values (≥97%) were observed for all enantiomers.

Configurational study was performed through CD and NOESY ^{1}H NMR spectra, by comparing the enantiomers (−)-**6e** and (−)-**6k** with (*S*)-tifluadom, the absolute configuration of which was determined by X-ray crystallographic analysis of its *p*-toluenesulfonic acid salt.[30] As already reported,[23] on the basis of the CD curves, the (S) absolute configuration of (+) tifluadom has also been proposed for (−)-**6e** and (−)-**6k**, because of the sequence of substituents around the stereogenic center, which is the same for all three enantiomers.

Additional analysis by ^{1}H NMR spectroscopy confirmed the configuration assignment. On the basis of the cross-peaks of the NOESY spectra, we could determine which protons are close to each other in the space for all compounds and, consequently, the configuration of the chiral center.[23]

Biology. Binding experiments of the title compounds to human cloned opioid receptors were performed in membranes prepared from HEK-293 (human embryonic kidney) or CHO (Chinese hamster ovary) cells stably expressing κ- (HEK-293), μ-, or δ- (CHO) opioid receptors, while binding studies on the native receptor were carried out in guinea pig brain homogenate, as previously described.[18]

A stable expression of μ-(h-MOR), δ-(h-DOR), and κ-(h-KOR) receptors has been performed in house, using pCDN vectors as described by Kotzer et al.[31]

The highly potent and specific radioligands [^{3}H]-[D-Ala^2,Mephe^4,Gly-ol^5]enkephalin ([^{3}H]-DAMGO), [^{3}H]-[D-Ala^2,D-Leu^5]enkephalin ([^{3}H]-DADLE), and [^{3}H]-U-69593 were used to label μ-, δ,- and κ-opioid receptors, respectively.[18,31] The results are reported in Table 1.

The potential antinociceptive and antiamnesic properties of compounds **6e** and **6i** were investigated by means of the hot-plate and passive avoidance test in mice, respectively.

Results and Discussion

Binding Studies. The most impressive result obtained from the binding studies is that this series of 2-[2-(acylamino)ethyl]-1,4-benzodiazepine derivatives binds the human cloned κ-opioid receptor subtype very tightly. Indeed, almost all the ligands within this class show subnanomolar K_i values, and the least potent compound **6o** shows, in any case, an affinity in the low nanomolar range. Comparison of the affinities obtained in the human cloned κ-receptor with the corresponding ones obtained in native guinea pig κ-receptor suggests that human cloned κ-receptor is less effective in discriminating the substitution pattern than the native guinea pig κ-receptor. In fact, the K_i values range from 0.25 to 13.6 nM in the case of the human cloned κ-receptor, while a wider range (0.19−296 nM) is observed in the case of native guinea pig κ-receptor. In particular, the human κ-receptor appears to be more tolerant in accommodating the additional steric bulk. For example, 7-chloro derivatives **6k**−**m** show κ-opioid affinities about an order of magnitude lower than the corresponding unsubstituted derivatives **6e**,**h**,**i** when the native guinea pig receptor is considered, while they show comparable affinities when the human cloned receptor is considered.

Table 1. Receptor Binding Affinities of 2-[(Acylamino)ethyl]-1,4-benzodiazepine Derivatives **6a**−**o**

						K_i (nM) ± SEM[a]					
						κ_1		μ		δ	
compd	X	Y	R_1	R_2	R_3	guinea pig[b]	human[c]	guinea pig[b]	human[c]	guinea pig[b]	human[c]
6a	H	H	H	H	thiophen-2-yl	1.74 ± 0.46	0.45 ± 0.05				
6b	H	H	H	H	phenyl		0.25 ± 0.05				
6c	H	H	H	H	2′- fluorophenyl		0.53 ± 0.14				
6d	H	H	H	H	4′-fluorophenyl		0.28 ± 0.04				
6e	H	H	CH_3	H	thiophen-2-yl	0.50 ± 0.10	0.58 ± 0.20	6.42 ± 0.96	9.4 ± 1.6	105 ± 48	93.9 ± 12
(*S*)-**6e**	H	H	CH_3	H	thiophen-2-yl	0.19 ± 0.03	0.43 ± 0.09		9.2 ± 3.6		63.2 ± 9.0
(*R*)-**6e**	H	H	CH_3	H	thiophen-2-yl	2.46 ± 0.13	1.28 ± 0.21		54.8 ± 11		544 ± 36
6f	H	OCH_3	CH_3	H	thiophen-2-yl	116 ± 15.9	3.77 ± 0.73				
6g	H	H	CH_3	CH_3	thiophen-2-yl	25.7 ± 2.2	4.34 ± 0.66				
6h	H	H	CH_3	H	2′-fluorophenyl	1.03 ± 0.42	0.36 ± 0.02				
6i	H	H	CH_3	H	4′-fluorophenyl	0.56 ± 0.10	0.30 ± 0.04				
6j	H	H	CH_3	H	4′-nitrophenyl		0.47 ± 0.04				
6k	Cl	H	CH_3	H	thiophen-2-yl	8.84 ± 1.47	0.70 ± 0.08	69.4 ± 15	26.3 ± 2.5	>1000	494 ± 34
(*S*)-**6k**	Cl	H	CH_3	H	thiophen-2-yl	4.52 ± 0.86	0.69 ± 0.21		27.4 ± 1.2		451 ± 6.0
(*R*)-**6k**	Cl	H	CH_3	H	thiophen-2-yl	6.55 ± 1.3	0.79 ± 0.21		33.2 ± 3.0		750 ± 42
6l	Cl	H	CH_3	H	2′-fluorophenyl	17.9 ± 6.44	1.52 ± 0.18				
6m	Cl	H	CH_3	H	4′-fluorophenyl	4.74 ± 1.33	0.55 ± 0.03				
6n	Cl	H	CH_3	H	4′-chlorophenyl	35.0 ± 5.1	1.31 ± 0.17				
6o	Cl	H	CH_3	H	indol-2-yl	296 ± 37	13.6 ± 2.56				
5						0.78 ± 0.19	0.37 ± 0.02	1.93 ± 0.08	3.0 ± 0.2	15.3 ± 1.71	69.0 ± 4.8
(*S*)-**5**							0.17 ± 0.04		1.5 ± 0.3		27.8 ± 4.7
(*R*)-**5**							0.71 ± 0.26		24.8 ± 2.0		438 ± 42
U-69593						1.89 ± 0.29	1.11 ± 0.13	1880 ± 324	>1000	>10 000	>1000
morphine						151 ± 10.2	64 ± 10	3.0 ± 0.3	3.0 ± 0.3	456 ± 57	299 ± 8
naltrindole						10.2 ± 1.5	4.4 ± 0.5	14.7 ± 3.6	7.2 ± 1.7	0.16 ± 0.04	0.24 ± 0.02

[a] Each value is the mean ± SEM of three independent experiments. [b] Native receptor from guinea pig. [c] Human cloned receptor.

From another viewpoint, 7-chloro derivatives **6k**−**o** show the human κ-receptor affinities to be about an order of magnitude higher than those shown for the native guinea pig κ-receptor, while unsubstituted derivatives **6e**,**h**,**i** show very similar affinities for both receptor subtypes. In a similar way, the introduction of either a methoxy substituent in position 6 of the 1,4-benzodiazepine nucleus or a methyl group on the amide nitrogen atom has more dramatic effects on the native guinea pig κ-receptor affinity than those shown on the human cloned κ-receptor. Interestingly, nor-derivatives **6a**,**c**,**d** show human κ-receptor affinities very similar to those shown by the corresponding 1-methyl derivatives **6e**,**h**,**i**, suggesting that the methyl group in position 1 of 1,4-benzodiazepine nucleus of this class of κ-receptor ligands does not play a key role in the interaction with the receptor and the most potent ligand of the class (compound **6b**) belongs to this small subseries of nor-derivatives.

Stereoselectivity. Finally, the binding studies reveal that compound **6e** interacts in the same stereoselective manner (the eutomer shows (*S*)-configuration as in the case of tifluadom) with all the opioid receptor subtypes evaluated showing eudismic ratios in the range of 12.95−2.97 (κ guinea pig, 12.95; κ human, 2.97; μ human, 5.95; δ human, 8.61). On the other hand, 7-chloro analogue **6k** binds the same opioid receptor subtypes with apparently absent stereoselectivity, suggesting that the 7-chloro substituent plays an important role in the interaction modalities.

In Vivo Biological Activity. Compounds **6e** and **6i** produced an increased pain threshold in the mouse hot-plate test after po (100 mg kg^{-1}) administration, as shown in Figure 1. The antinociceptive effect of **6e** and **6i** showed a peak 15 min after injection and then slowly diminished (see Supporting Information). The antinociceptive effect of **6e** and **6i** (100 mg kg^{-1} po) was antagonized by pretreatment with the κ-opioid antagonist n-BNI (1 nmol per mouse icv), injected 4 h before the test (Figure 1).

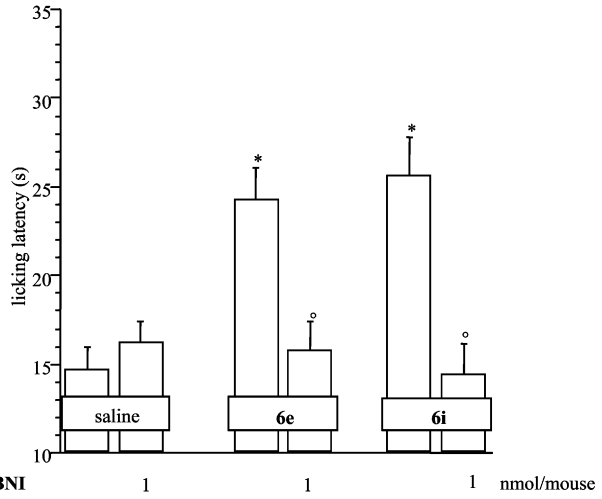

Figure 1. Antinociceptive effect of **6e** (100 mg kg^{-1} po) and **6i** (100 mg kg^{-1} po) in the mouse hot-plate test. The licking latency values reported in the figure were recorded 15 min after administration of **6e** and **6i**. Vertical lines represent sem; *P < 0.05 in comparison with saline-group; °P < 0.05 as compared with the corresponding antinociceptive compound.

These results emphasize the importance of the κ-opioid receptor activation in the inhibition of pain perception. Previous literature data reported that the κ-opioid agonists U-50,488H, TRK-820, and dynorphin A-(1−13) can induce antinociception in rats against mechanical, thermal, and chemical noxious stimuli.[32−35]

The κ-opioid receptor antagonist n-BNI (0.49 μg per mouse icv), injected immediately after the training session, produced amnesia in the passive-avoidance test.[36] This effect was obtained after intracerebroventricular administration, indicating that the blockade of κ-opioid receptors causes a centrally mediated memory impairment.

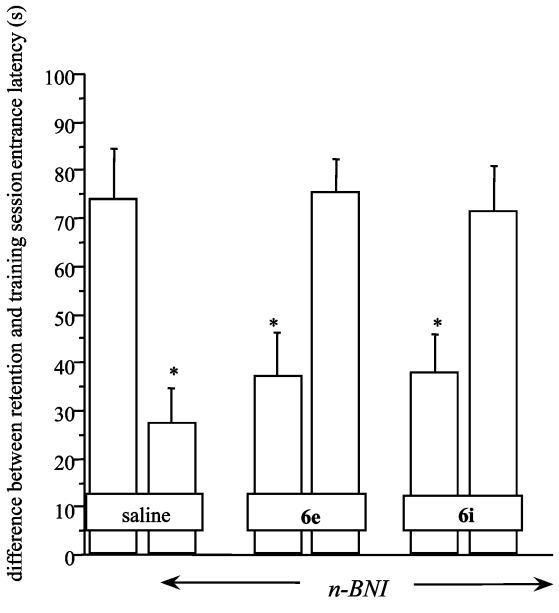

Figure 2. Antiamnesic effect of **6e** (100 mg kg^{-1} po) and **6i** (50 mg kg^{-1} po) in the mouse passive avoidance test. nor-Binaltorphimine hydrochloride (n-BNI) was injected icv, at the dose of 0.49 μg per mouse immediately before the training session. Vertical lines represent sem; *P < 0.05 in comparison with the saline group.

The deficits in passive avoidance behavior induced by n-BNI were prevented by pretreatment with the κ-opioid receptor agonists **6e** (100 mg kg^{-1} po) and **6i** (50 mg kg^{-1} po), administered 20 min before the training session, as shown in Figure 2. Both of the κ-opioid agonists enhanced the entrance latency up to a value comparable to that produced in control animals. Compounds **6e** and **6i** were completely ineffective at 50 and 10 mg kg^{-1} po, respectively (Figure 2).

Compounds **6e** and **6i**, when given alone at the highest doses, had no effect on mouse passive avoidance test in comparison with saline-treated mice (Figure 2). No statistically significant difference among the entrance latencies for each compound tested in the training session of the passive avoidance test was observed (Supporting Information).

These experimental results are in agreement with previous data reporting that the κ-opioid agonist dynorphin A-(1−13) reverts the scopolamine- and pirenzepine-induced memory impairment of step-down type passive avoidance response and spontaneous alternation performance.[37] Dynorphin A-(1−13) also reduces the amnesia induced by β-amyloid peptide-(25−35)[38] and cycloheximide,[39] a protein synthesis inhibitor in a mouse passive avoidance paradigm. Furthermore, U-50,488H, another κ-opioid agonist, has been reported to revert mecamylamine-induced memory impairment in mice and rats.[40−41]

The κ-opioid receptor agonists investigated, at the highest doses used, did not modify the animals' gross behavior. Nor did these compounds impair motor coordination or modify locomotor and inspection activity (see Supporting Information). We can, thus, assume that the effects produced by κ-opioid receptor agonists were not imputable to compromised viability.

In conclusion, the experimental data obtained by the use of two new and selective κ-opioid agonists, **6e** and **6i**, indicate that activation of κ-opioid receptors increases the pain threshold as well as improving pharmacologically induced cognitive deficits. These results confirm the important role played by κ-opioid receptors in the regulation of both pain perception and memory processes. On these bases, the κ-opioid agonists could be clinically useful for the relief of algic pathologies or for the treatment of cognitive disorders.

Computational Simulations. Comparison between the "Old" and "New" Model of the κ-Opioid Receptor. The results obtained in our previous paper,[18] published in 1996, have been obtained by a quantitative analysis of receptor docking simulations. The model of the guinea pig transmembrane (TM) receptor domain was based on both the bacteriorhodopsin structure[42] and on the helical wheel projection model proposed by Baldwin.[43] As can be noted from the sequence alignment reported in Figure 3, the differences in the TM domain between the human and guinea pig sequences consist only of four conservative mutations in helices 4, 5, and 6, while most of the differences are located in the N-terminal tail.

The zones selected as TM portions in the "old" model are highlighted in Figure 3 and can be easily compared to the TM domain of bovine rhodopsin, as shown by the crystal structure, and to those of the "new" model, evaluated after molecular dynamics and energy refinement of the averaged receptor structure. In the old model the helices were, in general, shorter, and by taking into account the uncertainty (4 aa) manifested by secondary structure prediction algorithms in locating the starting and ending points of α-helices,[44] the only significant differences are observed in the C-term portion of helix 3, and the N-term portion of helices 5 and 6.

In addition, the packing and mutual positions of the TMs are significantly different for the new and old models. However, the residues that were considered to be part of the binding site in our previous paper overlap very well, as can be appreciated in Figure 4 (top). They are **D138**, **N141**, and M142, in helix 3; W287, I290, **H291**, and I294, in helix 6; G319, **Y320**, N322, and S323 in helix 7. Some of these residues (reported in bold capitals in the text and in Figure 3) have been mutated into the opioid receptor superfamily. In particular, **D138** has been demonstrated to be involved both in agonist/antagonist binding and in signal transduction in κ-opioid receptor and several other GPCRs (GPCR family; a point mutation database, GRAP).[45] Mutation of the residue corresponding to **N141** in the δ-receptor (N150A) suggests that it may normally hinder the binding of opioid agonists.[46] The conserved **H291** in helix 6 has been found to be critical in both agonist and antagonist binding in the μ-receptor.[46] Mutation of **Y320** in the μ-receptor (Y326F) showed that it may be critical for opioid receptor binding, affecting the binding of agonists and antagonists, both opioid peptides and alcaloids.[46]

κ_1-Ligand Complexes and Linear Regression Analysis vs Binding. The energies for the κ_1-ligand complexes obtained as described in the Computational Methodology section, are reported in Table 2, together with the experimental binding affinities (pK_i). The

Figure 3. Sequence alignment of the bovine rhodopsin (b-OPSD), human k-opioid (h-OPRk), guinea pig *κ*-opioid (gp-OPRk), human *δ*-opioid (h-OPR*δ*), and human *μ*-opioid (h-OPR*μ*) receptors. The zones of the sequences selected as transmembrane domains are boxed, while the α-helices in the b-OPSD, as detected by the crystal structure, are shadowed. The residues of the h-OPRk that are believed to be part of the binding site in this study are highlighted and among these those that have been demonstrated to be important for ligand interaction by point mutation are reported in bold.

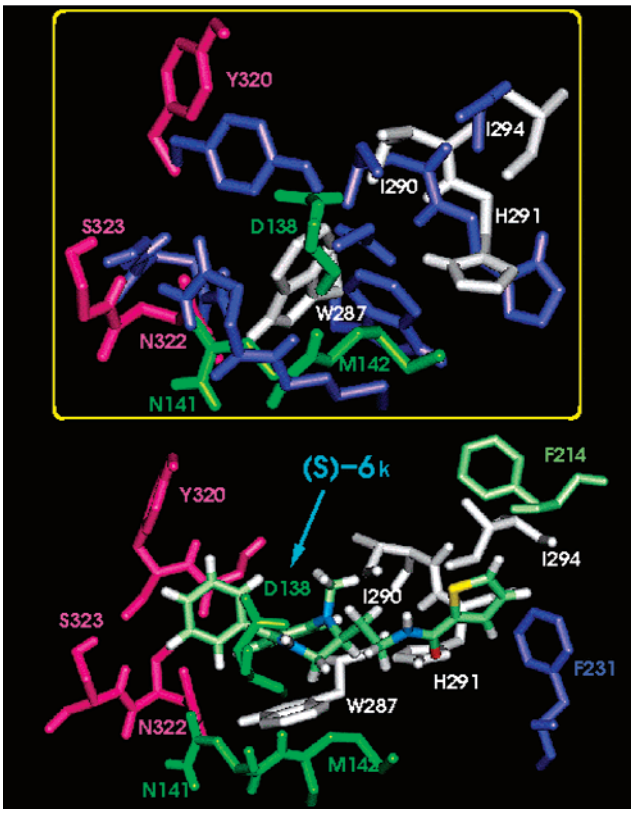

Figure 4. Superimposition of the amino acids that are believed to constitute the binding site in the "old" (blue) and "new" (in colors) models are reported at the top of the figure. Details of the interaction of the (*S*)-**6k** ligand with the human receptor (bottom) binding sites residues: the residues belonging to helix 3, helix 5, helix 6, and helix 7 are reported in green, blue, white and pink, respectively. The F214 (light green) belongs to the loop connecting helix 4 with helix 5.

Table 2. Experimental Binding Constants and Computed Energy Descriptors (kcal/mol) for the Ligand−κ_1 Receptor Interactions

compd[a]	pK_i κ_1-human	BE	IE_{k-L}	E^d_L	E^d_k
6a	9.35	−37.54	−70.27	4.25	28.48
6b	9.60	−41.89	−73.94	3.68	28.37
6c	9.27	−41.19	−74.49	4.25	29.05
6d	9.55	−40.33	−73.82	3.84	29.65
(*S*)-**6e**	9.37	−38.77	−75.27	5.74	30.76
6f	8.42	−25.48	−70.44	6.32	38.64
6g	8.36	−25.11	−69.71	4.54	40.06
6h	9.44	−39.40	−72.19	6.11	26.68
6i	9.52	−43.08	−74.40	4.32	27.01
6j	9.32	−41.49	−76.55	4.94	30.12
(*S*)-**6k**	9.16	−37.23	−71.56	5.47	28.86
6l	8.81	−28.45	−74.58	5.86	40.27
6m	9.26	−38.73	−75.55	6.33	30.49
6n	8.88	−29.76	−76.78	5.79	41.23
6o	7.87	−20.58	−70.55	6.33	43.64
(*S*)-**5**	9.77	−41.44	−74.31	5.79	27.08

[a] For racemic compounds **6a**−**d**,**f**−**j**,**l**−**o**, configuration *S* was used in the docking studies.

variation in the measured binding constants is well-explained by the computed binding energies (BE), which take into account the ligand−receptor interaction energy (IE_{k-L}) and the mutual conformational adjustment of the ligand (E^d_L) and of the receptor (E^d_k) upon binding. The quantitative relationship obtained between the binding affinity data values and the computed binding energies for the ligands considered is shown in Figure 5.

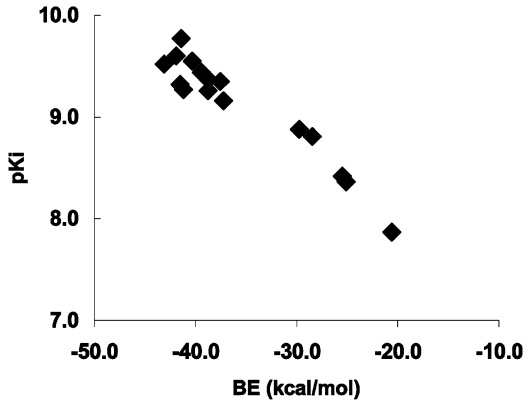

Figure 5. Correlation between the binding affinity values and the calculated binding energies for the minimized ligand−receptor complexes. The linear regression is $pK_i = 6.65\ (\pm 0.19) - 0.07\ (\pm 0.005)BE$, $n = 16$, $r^2 = 0.92$, $s = 0.15$, where n is the number of the compounds, r is the correlation coefficient, s is the standard deviation and the values in parentheses give the 95% confidence intervals.

As expected from the similarity observed in the spatial position of the old and new receptor binding site residues, the binding modalities of the ligands involve the same residues spotted in our previous model.[18] This is shown in Figure 4 (bottom), where the details of the interaction of the (*S*)-**6k** ligand with the human receptor are reported.

In agreement with our previous findings,[18] the changes in the potential energy of the receptor upon formation of the complexes are mainly responsible for the correlation obtained (Table 2). In fact, inspection of the interaction energy values reveals that their variation is disorganized and varies within a small interval. This implies that repulsion forces play the most important role in discriminating between the compounds considered, and a reorganization of the receptor architecture is needed in order to accommodate the ligands.

Analysis of the molecular dynamics trajectories of the ligand−receptor complexes shows that the receptor reorganization is mainly triggered by Pro15 in helix 6, positioned just below the putative active site, which allows the kinking of the C-terminal part of the helix away from the core of the receptor. The extent of this structural change depends on the structural features of the ligands and influences the overall packing of the bundle. This finding is in full agreement with the results obtained by mapping of the residue in the sixth TM domain of the κ-, δ-, and μ-opioid receptor subtypes, which are accessible in the binding-site crevices by the substituted cysteine accessibility method.[47]

The flexibility of this region involves also the H-bonding observed between residue **E298** of helix 6 and **Y312** of helix 7. The **E297K** mutation[48] has demonstrated the importance of this residue for the binding of the nor-BNI ligand. Since the ligands used in our study are of much smaller size, they bind deeply in the TM domain and do not interact directly with residue **E298**, which, however, might be the second key point for the regulation of the overall shape of the binding pocket and might contribute to determine the receptor selectivity. In fact, **E298** and **Y312** are not conserved in the δ- and μ- receptors, being W (δ) and K (μ) and L (δ) and W (μ), respectively (Figure 3).

The results obtained showed that the "new" computational model satisfactorily explains the structure−activity relationships observed and provides additional structural interpretation for the results of published mutagenesis experiments.

Experimental Section

Melting points were determined in open capillaries on a Gallenkamp apparatus and are uncorrected. Microanalyses were carried out using a Perkin-Elmer 240 C elemental analyzer. ^{1}H NMR spectra were recorded on a Bruker AC 200 spectrometer; the values of the chemical shift are expressed in ppm and the coupling constants (*J*) in hertz. Merck silica gel 60 (230−400 mesh) and Chromabond Florisil 6 mL/1000 mg (Superchrom) were used for column chromatography. Merck DC-Platten F 254 was used for TLC. Mass spectra were recorded on a VG 70−250 S spectrometer. Microanalyses were performed by the Dipartimento Farmaco Chimico Tecnologico dell'Università di Siena, while mass spectra were performed by Centro di Analisi e Determinazioni Strutturali, Università di Siena. Commercial chemicals were used without further purification, except for solvents, which were purified and dried, where appropriate, before use by standard methods.

HPLC was performed on a Gilson (model 319) with an injection valve (Reodyne, model 7125) and a UV detector (Perkin-Elmer, model LC 95). Experimental data were analyzed with HPLC software (Gilson 715). UV spectra were recorded on a spectrophotometer (Perkin-Elmer, model 552). CD curves were measured on a dichrograph (Jasco, model J-710).

General Procedure for the Preparation of 2-[(Acylamino)ethyl]-1,4-benzodiazepine 6a−d. The 2-[(acylamino)ethyl]-1,4-benzodiazepines **6a**−**d** were synthesized following a previously described procedure.[18] Briefly, a suspension of the phthalimido derivative **10** (2.5 mmol) in MeOH (30 mL) treated with hydrazine 98% (1.21 mL, 25 mmol) was stirred at room temperature for 4 h, diluted with MeOH (20 mL), and filtered. The precipitate was discarded, and the filtrate was concentrated under reduced pressure. The residue was partitioned between CH_2Cl_2 (50 mL) and ice-cold aqueous dilute hydrochloric acid (10 mL). The organic layer was discarded, and the acidic aqueous solution was made alkaline with ice-cold 3 M sodium hydroxide solution. The reaction product was then extracted with CH_2Cl_2 and the organic phase washed with brine until neutral and dried over $MgSO_4$. Evaporation under reduced pressure gave pure 2,3-dihydro-2-(2-aminoethyl)-5-phenyl-1*H*-1,4-benzodiazepine in 70% yield as a colorless oil, which was dissolved into dry THF (12 mL) and treated in succession, after cooling at 0 °C, with Et_3N (245 μL) and the appropriate acyl chloride (1.76 mmol) dissolved into dry THF (3 mL). The ice bath was removed, and the reaction mixture was stirred overnight at room temperature and then diluted with ethyl acetate (100 mL). The organic layer was washed with a saturated $NaHCO_3$ solution (2 × 30 mL) and brine, dried over $MgSO_4$, and concentrated under reduced pressure to give a crude product which, after purification by column chromatography, afforded the respective acylamino derivative.

2,3-Dihydro-2-[[(2-thienylcarbonyl)amino]ethyl]-5-phenyl-1*H*-1,4-benzodiazepine (6a). This compound was prepared in 35% yield starting from **10** according to the procedure, using 2-thienylcarbonyl chloride in the second step as acylating agent and purifying by flash chromatography (EtOAc−*n*-hexane, 70:30, v/v) to obtain a light yellow oil. A further flash chromatography afforded an analytical sample. ^{1}H NMR ($CDCl_3$): δ 1.77−1.99 (m, 2H), 3.26−3.41 (m, 1H), 3.72−3.93 (m, 3H), 4.05−4,14 (m, 1H), 4.65 (bs, 1H, disappeared with D_2O), 6.74 (t, 1H, *J* = 7.1), 6.82 (d, 1H, *J* = 7.8), 6.95−7.07 (m, 2H), 7.19−7.55 (m, 9H). MS (EI): *m*/*z* 375 (M^+, 25). Anal. ($C_{22}H_{21}N_3OS$): C, H, N.

2,3-Dihydro-2-[[(benzoyl)amino]ethyl]-5-phenyl-1*H*-1,4-benzodiazepine (6b). This compound was prepared in 54% yield starting from **10** according to the general procedure and using benzoyl chloride in the second step as acylating agent. After purification by flash chromatography (EtOAc−MeOH, 90:10, v/v) an orange glassy solid was obtained. ^{1}H NMR ($CDCl_3$): δ 1.80−2.05 (m, 2H), 3.31−3.49 (m, 1H), 3.72−3.97 (m, 3H), 4.05−4,14 (m, 1H), 4.68 (bs, 1H, disappeared with D_2O), 6.72−6.89 (m, 2H), 7.03 (d, 1H, *J* = 8.3), 7.21−7.58 (m, 10H), 7.82 (d, 2H, *J* = 7.05). MS (FAB): *m*/*z* 370 (M + 1). Anal. ($C_{24}H_{23}N_3O$): C, H, N.

2,3-Dihydro-2-[[(2-fluorobenzoyl)amino]ethyl]-5-phenyl-1*H*-1,4-benzodiazepine (6c). This compound was prepared in 21% yield starting from **10** according to the general procedure, using 2-fluorobenzoyl chloride in the second step as acylating agent and purifying by flash chromatography (EtOAc−MeOH, 90:10, v/v) to obtain a yellow solid. A recrystallization from cyclohexane gave an analytical sample melting at 97−98 °C. ^{1}H NMR ($CDCl_3$): δ 1.81−2.05 (m, 2H), 3.31−3.46 (m, 1H), 3.76−4.16 (m, 4H), 4.65 (bs, 1H, disappeared with D_2O), 6.73 (t, 1H, *J* = 7.4), 6.85 (d, 1H, *J* = 7.9), 6.98−7.55 (m, 10H) 8.03−8.11 (m, 1H). MS (EI): *m*/*z* 387 (M^+, 22). Anal. ($C_{24}H_{22}FN_3O$): C, H, N.

2,3-Dihydro-2-[[(4-fluorobenzoyl)amino]ethyl]-5-phenyl-1*H*-1,4-benzodiazepine (6d). This compound was prepared in 58% yield starting from **10** according to the general procedure, using 4-fluorobenzoyl chloride in the second step as acylating agent and purifying by flash chromatography (EtOAc−*n*-hexane, 70:30, v/ v) to obtain a light yellow oil. ^{1}H NMR ($CDCl_3$): δ 1.85−1.97 (m, 2H), 3.36−3.48 (m, 1H), 3.73−3.81 (m, 2H), 3.93 (dd, 1H, *J* = 3.9, 11.7), 4.08−4.21 (m, 1H), 4.64 (bs, 1H, disappeared with D_2O), 6.72−6.83 (m, 2H), 6.99−7.17 (m, 2H), 7.21−7.45 (m, 6H), 7.50−7.56 (m, 2H), 7.77−7.84 (m, 2H). MS (EI): *m*/*z* 387 (M^+, 19). Anal. ($C_{24}H_{22}FN_3O$): C, H, N.

(*Z*)-2,3-Dihydro-2-[(ethoxycarbonyl)methylene]-5-phenyl-1*H*-1,4-benzodiazepine (7). This compound was prepared as previously described[18] and its analytical and spectral data were consistent with those reported therein.

Ethyl (2,3-Dihydro-5-phenyl-1*H*-1,4-benzodiazepine)-2-acetate (8). This compound was prepared following the procedure previously described.[18] A solution of compound **7** (1.0 g, 3.2 mmol) in TFA (15 mL) was stirred under N_2 atmosphere and cooled in an ice bath. The solution was treated with triethylsilane (0.74 g, 6.4 mmol) added over a period of 5 min. The ice bath was removed, and the stirring was continued for 30 min. The mixture was then poured onto crushed ice, made alkaline by addition of ammonia, and extracted with CH_2Cl_2. The extracts were combined, dried (Na_2SO_4), and evaporated under reduced pressure. The residue was purified by column chromatography (CH_2Cl_2–EtOAc, 95−5 v/v), and **8** was obtained as a thick yellow oil. Further purification by chromatography afforded an analytical sample as a colorless oil. ^{1}H NMR ($CDCl_3$): δ 1.25 (t, 3H, *J* = 7.4), 2.60−2.85 (q, 2H), 3.65−3.91 (m, 2H), 4.05−4.25 (m, 2H), 4.38−4.57 (bs, 2H, 1H disappeared with D_2O), 6.74−6.89 (m, 2H), 7.0−7.10 (m,1H), 7.20−7.28 (m, 1H), 7.30−7.42 (m, 3H), 7.51 (dd, 2H, *J* = 1.5, 7.5). Anal. ($C_{19}H_{20}N_2O_2$): C, H, N.

2,3-Dihydro-2-(2-hydroxyethyl)-5-phenyl-1*H*-1,4-benzodiazepine (9). To a stirred suspension of lithium aluminum hydride (3.2 mmol) in anhydrous THF (15 mL) was added dropwise a solution of **8** (1.5 mmol) in dry THF (15 mL). After stirring under argon atmosphere for 15 min, the excess of lithium aluminum hydride was decomposed by careful addition of H_2O (1 mL). The organic material was filtered off and washed with THF. The filtrate was dried over Na_2SO_4, filtered, and evaporated under reduced pressure. The crude product was purified by flash chromatography (EtOAc) to give **9** in 83% yield, as a yellow oil. An analytical sample was obtained by further column chromatography. ^{1}H NMR (DMSO): δ 1.72−1.98 (m, 2H), 3.49 (bs, ^{1}H, disappeared with D_2O), 3.67−3.80 (m, 2H), 3.88 (dd, 2H, *J* = 3.1; 11,0), 4.17−4.21 (m, ^{1}H), 4.28 (bs, ^{1}H, disappeared with D_2O), 6.70−6.81 (m, 2H), 7.01 (d, ^{1}H, *J* = 7.4), 7.18−7.39 (m, 4H), 7.53 (dd, 2H, *J* = 1.5, 7.5). Anal. ($C_{17}H_{18}N_2O$): C, H, N.

2,3-Dihydro-2-(2-phthalimidoethyl)-5-phenyl-1*H*-1,4-benzodiazepine (10). This compound was prepared in 87% yield as previously described[18] and purified by flash chroma-

tography (*n*-hexanes−EtOAc, 65:35, v/v) to obtain a light yellow oil. Further column chromatography afforded an analytical sample. ^{1}H NMR ($CDCl_3$) δ 1.94−2.04 (m, 2H), 3.71−4.01 (m, 5H), 4.75 (bs, 1H, disappeared with D_2O), 6.76 (t, 1H, $J = 7.7$), 6.88 (d, 1H, $J = 8.1$), 7.0 (d, 1H, $J = 7.6$), 7.20−7.29 (m, 1H), 7.32−7.38 (m, 3H), 7.52 (dd, 2H, $J = 1.3, 6.6$), 7.69−7.75 (m, 2H), 7.80−7.87 (m, 2H). Anal. ($C_{25}H_{21}N_3O_2$) C, H, N.

Chiral Chromatographic Resolution. All chemicals and solvents were of analytical grade or HPLC grade. UV spectra were measured on a Beckman DU-7000 spectrometer. Specific rotations (α) were measured on a Jasco DIP-1000 photoelectric polarimeter (0.5 dm cell, sodium lamp). Circular dichroism was recorded on a Jasco J-710 dichrograph. The analytical chiral resolutions were performed by liquid chromatography on Chiralcel OJ-R and Chiralpak AD columns (0.46 × 25 cm) from Daicel Chemical Industries, Tokyo, Japan. The chiral stationary phases of these columns were, respectively, cellulose tris-4-methylbenzoate or amylose tris-3,5-dimethylphenylcarbamate, coated on a 5 μm silica gel substrate. Semipreparative resolution was accomplished by a Chiralpak AD column (2 × 25 cm, 10 μm). The HPLC system consisted of two Gilson pumps (model 306), a Reodyne injector (model 7125, 20 μL or 3 mL sample loop, respectively, for analytical or semipreparative resolutions), and a Gilson (model 119) UV detector at double wavelength. Experimental data were analyzed with Gilson 715 software. All chromatographic separations were performed at room temperature. The enantiomers of **6e** and **6k** were completely resolved on Chiralpak AD column by means of *n*-hexane/isopropyl alcohol 85/15 as eluent. The enantioselectivity (α) and the resolution (R_s) were 1.87 and 1.26 for **6e** and 1.18 and 2.18 for **6k**. A semipreparative process was carried out with the same chiral stationary phase on a 250 × 20 mm column, eluting with *n*-hexane/isopropyl alcohol 95/5. The chromatographic process was repeated every 45 min by injection of 2 mL of the sample solution ($c = 2-3$ mg solute/mL of *n*-hexane 70/isopropyl alcohol 30 mixture). Pure enantiomers were properly recovered by partition of the eluate according to the profile of the chromatogram. In this way about 25 mg of the chiral compounds was obtained.

Computational Methodology. Comparative Modeling of the Human κ-Opioid Receptor. The recently determined 2.8 Å X-ray structure of rhodopsin[24] was used to build the human κ-opioid receptor model. The sequence alignment used as input for the Modeler[49] program is reported in Figure 3 and was obtained by Clustalw[50] multiple sequence alignment of bovine rhodopsin and human κ-, δ-, and μ-opioid receptor sequences. Among the 50 models obtained by randomizing the Cartesian coordinates, allowing a deviation of ±4 Å, we selected the one showing the lowest restraint violations and the lowest number of main chain and side chain bad conformations. The quality of the models was checked by using the protein health module of the program Quanta98 (Accelrys, San Diego, CA). Polar hydrogens were added to the selected model, and energy minimization and dynamics were carried out by means of the CHARMM program[51] following a standard procedure consisting of 50 steps of steepest descent, followed by a conjugate gradient minimization until the root mean square gradient of the potential energy was lower than 0.001 kcal/mol Å. The united atom force field parameters, a distance-dependent dielectric term ($\epsilon = 4r$), and a 12 Å nonbonded cutoff were employed. During dynamics the lengths of the bonds involving hydrogen atoms were constrained according to the SHAKE algorithm[52] allowing an integration time step of 0.001 ps. Moreover, weak harmonic constraints (30 kJ/mol per Å) were applied between the backbone oxygen atoms of residue i and backbone nitrogen atom of residue $I + 4$ by means of the NOE facility in the CHARMM program[51] in order to preserve the helical structure.

The structures were thermalized to 300 K with 5 °C rise per 6000 steps by randomly assigning individual velocities from the Gaussian distribution. After heating, the systems were allowed to equilibrate until the potential energy versus time was approximately stable (34 ps). Velocities were scaled by a single factor. An additional 10 ps period of equilibration with no external perturbation was run. Time-averaged structures were then determined over the last 200 ps of each simulation. Data were collected every 0.5 ps.

Building and Refinement of the Ligand−Receptor Complexes. The ligands were manually docked into the minimized average structure of the receptor, the main criteria being the formation of a charge-reinforced hydrogen bond between the protonated nitrogen atom of the ligands and the **D138** residue of helix 3 and the formation of a hydrogen bond between the carbonyl oxygen atom of the ligand and the **H291** residue of helix 6. The procedure used is described in detail in our previous paper.[18]

The binding energies (BE) of the minimized ligand−receptor complexes were calculated according to the following equation:[53] $BE = IE_{k-L} + E^d_L + E^d_k$ where, IE_{k-L} is the total interaction energy between the receptor and the ligand, E^d_L is the distortion energy of the ligand calculated with respect to the optimized energy of the free molecule, and E^d_k is a measure of the conformational energy change in the receptor induced by ligand binding. Ligand and receptor distortion energies were obtained by minimizing the ligand and the receptor separately, resulting in the same geometry in each minimized complex.

In Vitro Binding Assays. Binding experiments of the title compounds to human cloned opioid receptors were performed in membranes prepared from CHO (Chinese hamster ovary) or HEK-293 (human embrionic kidney) cells stably expressing μ- or δ-(CHO) or κ- (HEK-293) opioid receptors. Native receptor studies were carried out in guinea pig brain homogenate, as previously described.[18]

A stable expression of μ- (h-MOR), or δ- (h-DOR), and κ- (h-KOR) receptors has been performed in house, using pCDN vectors as described by Kotzer et al.[31]

Membranes were prepared by lysis in hypotonic phosphate-buffer according to the method described by Scheideler and Zukin.[54] The highly potent and specific radioligands [^{3}H]-[D-Ala^2,Mephe^4,Gly-ol^5]enkephalin ([^{3}H]-DAMGO, 50 Ci/mmol, New England Nuclear, Bruxelles, Belgium), [^{3}H]-[D-Ala^2,D-Leu^5]enkephalin ([^{3}H]-DADLE, 50 Ci/mmol, New England Nuclear, Bruxelles, Belgium), and [^{3}H]-U-69593 (63 Ci/mmol, Amersham) were used to label μ-, δ- and κ-opioid receptors, respectively.[18,31]

Nonspecific binding was determined in the presence of 10 μM naloxone. Binding experiments to cloned receptors were performed in 25 mM monobasic potassium phosphate buffer containing 3 mM $MgCl_2$, pH 7.4, in polypropylene 96-deep-well plates.

Incubation was carried on for 60 min at 25 °C at the final volume of 0.5 mL (μ-assay) or 0.7 mL (δ- and κ-assay). The reaction was terminated by filtration using a Packard Filtermate harvester containing a GF/B Unifilter plate. After filtration the Unifilter plates were dried, each well was filled with 50 μL of Packard Microscint 30, and radioactivity counted by a Packard Topcount NXT.

Analysis of Binding Data. The binding parameters deriving from competition experiments (IC_{50} values) were calculated by nonlinear regression analysis using the RS/1 software.[55] The inhibition constants (K_i) were calculated from IC_{50} values using the Cheng and Prusoff equation.[56]

In Vivo Biological Tests. The potential antinociceptive and antiamnesic properties of compounds **6e** and **6i** were investigated by means of the hot-plate and passive avoidance test in mice, respectively.

Male Swiss albino mice (23−25 g) from the Morini (San Polo d'Enza, Italy) breeding farm were used. Fifteen mice were housed per cage (26 × 41 cm). The cages were placed in the experimental room 24 h before the test for acclimatization. The animals were fed a standard laboratory diet and tap water ad libitum and kept at 23 ± 1 °C with a 12 h light/dark cycle, light on at 7 a.m. All experiments were carried out in accordance with the European Community Council Directive of 24 November, 1986 (86/609/EEC) for experimental animal care. All efforts were made to minimize animal suffering and to reduce the number of animals used.

Hot-Plate Test. The method adopted was described by O'Callaghan and Holzman.[57] Mice were placed inside a stainless steel container, thermostatically set at 52.5 ± 0.1 °C in a precision water-bath from KW Mechanical Workshop (Siena, Italy). Reaction times (s), were measured with a stop-watch before and at regular intervals up to a maximum of 60 min after treatment. The endpoint used was the licking of the fore or hind paws. Those mice scoring below 12 and over 18 s in the pretest were rejected (30%). An arbitrary cutoff time of 45 s was adopted.

Passive-Avoidance Test. The test was performed according to the step-through method described by Jarvik and Kopp.[58] The apparatus consists of a two-compartment acrylic box with a lighted compartment connected to a darkened one by a guillotine door. As soon as they entered the dark compartment, the mice received a punishing electrical shock (0.15 mA, 1 s). The latency times for entering the dark compartment were measured in the training test and after 24 h in the retention test. For memory disruption, mice were ip injected with amnesic drugs immediately after termination of the training session. Compounds **6e** and **6i** were administered 20 min before the training session. Those mice scoring more than 60 s in the training session were rejected. The maximum entry latency allowed in the retention session was 180 s. The degree of memory recall of received punishment (electric shock) was expressed as the difference (Δ) between retention and training latencies.

Intracerebroventricular Injection Technique. Intracerebroventricular (icv) administration was performed under ether anaesthesia with isotonic saline as a solvent, according to the method described by Haley and McCormick.[59] During anaesthesia, mice were grasped firmly by the loose skin behind the head. A hypodermic needle (0.4 mm external diameter) attached to a 10 μL syringe was inserted perpendicularly through the skull and no more than 2 mm into the brain of the mouse, where 5 μL of drug was then administered. The injection site was 1 mm to the right or left from the midpoint on a line drawn through to the anterior base of the ears. Injections were performed randomly into the right or left ventricle. To ascertain that the drugs were administered exactly into the cerebral ventricle, some mice were injected with 5 μL of 1:10 diluted India ink and their brains were examined macroscopically after sectioning. The accuracy of the injection technique was evaluated and the percentage of correct injections was 95.

Drugs. nor-Binaltorphimine hydrochloride (n-BNI, purchased from RBI) was used.

The drug was dissolved into isotonic (NaCl 0.9%) saline solution (for icv administration) or dispersed into sodium carboxymethylcellulose 1% (for po administration) immediately before use. Drug concentrations were prepared so that the necessary dose could be administered in a volume of 5 μL per mouse by intracerebroventricular (icv) injection and 10 mL kg^{-1} by per os (po) injection.

Statistical Analysis. All experimental results are given as the means ± sem. The analysis of variance (ANOVA), followed by Fisher's protected least significant difference (PLSD) procedure for post-hoc comparison, was used to verify the significance between two means. The data were analyzed with the StatView software for the Macintosh (1992). *P* values of less than 0.05 were considered significant.

Acknowledgment. We acknowledge the contribution of Dr G. Giorgi (C.I.A.D.S., University of Siena, Italy) for the recording of mass spectra. Prof. S. D'Agata D'Ottavi's careful reading of the manuscript is also acknowledged. Financial support from CNR and Italian MIUR is acknowledged.

Supporting Information Available: Experimental details for the synthesis and the characterization of compounds **6** and their intermediates (chemistry, NMR, MS). This material is available free of charge via Internet at http://pubs.acs.org.

References

(1) Reisine, T.; Pasternak In Goodman and Gilman's *The Pharmacological Basis of Therapeutics*; Hardman, J. G., Limbird, L. E., Eds.; McGraw-Hill: 1996; pp 521−525.
(2) Tseng, L. F. Evidence for ϵ-Opioid Receptor-Mediated β-Endorphin-Induced Analgesia. *Trends Pharm. Sci.* **2001**, *22*, 623−629.
(3) Simon, E. J.; Gioannini, T. L. Opioid Receptor Multiplicity: Isolation, Purification and Chemical Characterization of Binding Sites. In *Handbook of Experimental Pharmacology*, 104/1; Herz A., Ed.; Springer-Verlag: Berlin, 1993; pp 3−26.
(4) B. N.; Cesselin, R.; Raghubir, R.; Reisine, T.; Braedley, P. B.; Portoghese, P. S.; Hamon M. International Union of Pharmacology. XII. Classification of Opioid Receptors. *Pharmacol. Rev.* **1996**, *48*, 567−592.
(5) Zimmerman, D. M.; Leander, J. D. Selective Opioid Receptor Agonists and Antagonists: Research Tools and Potential Therapeutic Agents. *J. Med. Chem.* **1990**, *33*, 895−902.
(6) Matthes, H. W. D.; Maldonado, R.; Simonin, F.; Valverde, O.; Slowe, S.; Kitchen, I.; Befort, K.; Dierich, A.; Le Meur, M.; Dollé, P.; Tzavara, E.; Hanoune, J.; Roques, B. P.; Kieffer, B. L. Loss of Morphine-Induced Analgesia, Reward Effect and Withdrawal Symptoms in Mice Lacking the μ-Opioid-Receptor Gene. *Nature* **1996**, *383*, 819−823.
(7) Sora, I.; Takahashi, N.; Funada, M.; Ujike, H.; Revay, R. S.; Donovan, D. M.; Miner, L. L.; Uhl, G. R. Opiate Receptor Knockout Mice Define μ Receptor Roles in Endogenous Nociceptive Responses and Morphine-induced Analgesia. *Proc. Natl. Acad. Sci. U.S.A.* **1994**, *94*, 1544−1549.
(8) Tao, P. L.; Hwang, C. L.; Chen, C. Y. U-50,488 Blocks the Development of Morphine Tolerance and Dependence at a Very Low Dose in Guinea Pigs. *Eur. J. Pharmacol.* **1994**, *256*, 281−286.
(9) Itoh, J.; Ukai, M.; Kameyama, T. Dynorphin A-(1−13) Potently Improves the Impairment of Spontaneous Alternation Performance Induced by the μ-Selective Opioid Receptor Agonist DAMGO in Mice. *J. Pharm. Exp. Ther.* **1994**, *269*, 15−21.
(10) Martin, W. R.; Eades, C. G.; Thompson, J. A.; Huppler. R. E.; Gilbert, P. The Effects of Morphine- and Nalorphine-like Drugs in the Non-Dependent and Morphine-Dependent Chronic Spinal Dog. *J. Pharm. Exp. Ther.* **1976**, *197*, 517−532.
(11) Szmuszkovicz, J.; Von Voightlander, P. F. Benzeneacetamide Amines: Structurally Novel Non-μ-Opioids. *J. Med. Chem.* **1982**, *25*, 1125−1126.
(12) Von Voigtlander, P. F.; Lahti, R. A.; Ludens, J. H. U-50,488: a Selective and Structurally Novel non-Mu (kappa) Opioid Agonist. *J. Pharm. Exp. Ther.* **1983**, *224*, 7−12.
(13) Endoh, T.; Tajima, A.; Izumimoto, N.; Suzuki, T.; Saitoh, A.; Suzuki, T.; Narita, M.; Kamei, J.; Tseng, L. F.; Mizoguchi, H.; Nagase, H. TRK-820, a Selective kappa Opioid Agonist, Produces Potent Antinociception in Cynomologus monkeys. *Jpn. J. Pharmacol.* **2001**, *85*, 282−290.
(14) Endo, T.; Nagase, H.; Suzuki, T.; Suzuki, T.; Tanaka, T.; Kawamura, K.; Kuraishi, Y.; Shiraki, K. Remedies for Neuropathic Pain and Model Animals of Neuropathic Pain. 2001, WO-00114383.
(15) Nagase, H.; Uchiumi, J.; Okano, K.; Kawamura, K.; Inada, H.; Togashi, H. Antipruritic for Cornea or Conjunctiva. 2001, JP-163784.
(16) Romer, D.; Buscher, H. H.; Hill, R. C.; Maurer, R.; Petcher, T. J.; Zeugner, H.; Benson, W.; Finner, E.; Milkowsky, W.; Thies, P. W. An Opioid Benzodiazepine. *Nature (London)* **1982**, *298*, 759−760.
(17) Chang, R. S. L.; Lotti, V. J.; Chen, T. B.; Keegan, M. E. Tifluadom, a *k*-Opiate Agonist, Acts as a Peripheral Cholecystokinin Receptor Antagonist. *Neurosci. Lett.* **1986**, *72*, 211−214.
(18) Cappelli, A.; Anzini, M.; Vomero, S.; Menziani, M. C.; De Benedetti, P. G.; Sbacchi, M.; Clarke, G. D.; Mennuni, L. Synthesis, Biological Evaluation, and Quantitative Receptor Docking Simulations of 2-[(Acylamino)ethyl]-1,4-benzodiazepines as Novel Tifluadom-like Ligands with High Affinity and Selectivity for κ-Opioid Receptors. *J. Med. Chem.* **1996**, *39*, 860−872.
(19) Petrillo, P.; Amato, M.; Tavani, A. The Interaction of the Two Isomers of the Opioid Benzodiazepine Tifluadom with μ, κ and δ Binding Sites and their Antinociceptive and Intestinal Effects in Rats. *Neuropeptides* **1985**, *5*, 403−406.
(20) Freye, E.; Boeck, G.; Schaal, M.; Ciaramelli, F. The Benzodiazepine (+)-Tifluadom (KC-6128), but not its Optical Isomers (KC-5911) Induces Opioid kappa Receptor-Related EEG Power Spectra and Evoked Potential Changes. *Pharmacology* **1986**, *33*, 241−248.
(21) Kley, H.; Scheidemantel, U.; Bering, B.; Muller, W. E. Reverse Stereoselectivity of Opiate and Benzodiazepine Receptors for the Opioid Benzodiazepine Tifluadom. *Eur. J. Pharmacol.* **1983**, *87*, 503−504.

(22) Meurisse, R. L.; Hevlen, L.; Leysen, J. E.; Meunier, J. C.; De Ranter, C. Radioligand Binding Profile of Enantiomers of Tifluadom Analogues for Opioid, CCK, and Central Benzodiazepine Receptors: Versatility of Benzodiazepine Skeleton. *Regul. Pept.* **1984**, *1*, 5347−5248.
(23) Azzolina, O.; Collina, S.; Linati, L.; Anzini, M.; Cappelli, A.; Scheideler M. A.; Sbacchi, M. Enantiomers of 2[(Acylamino)-ethyl]-1,4-benzodiazepiones, Potent Ligands of k-Opioid Receptor: Chiral Chromatographic Resolution, Configurational Assignment, and Biological Activity. *Chirality* **2001**, *13*, 606−612.
(24) Palczewski, K.; Kumasaka, T.; Hori, T.; Behnke, C. A.; Motoshima, H.; Fox, B. A.; Le Trong, I.; Teller, D. C.; Okada, T.; Stenkamp, R. E.; Yamamoto, M.; Miyano, M. Crystal Structure of Rhodopsin: A G-Protein-Coupled Receptor. *Science* **2000**, *289*, 739−745.
(25) Ghelardini, C.; Galeotti, N.; Bartolini, A.; Anzini, M.; Cappelli, A.; Vomero, S. Antiamnesic Effect of the Two Novel k-Opioid Agonists, VA 100 and VA 101, in the Mouse Passive Avoidance Test. *Drug Dev. Res.* **2001**, *54*, 12−18.
(26) Anzini, M.; Cappelli, A.; Vomero, S. Synthesis and Receptor Binding Studies of 2-Functionalized 1,4-Benzodiazepine Derivatives as Potential Metaclazepam-like Antianxiety Agents. *Farmaco* **1993**, *48*, 897−905.
(27) Anzini, M.; Garofalo, A.; Vomero, S. Syntheses of Functionalized Derivatives of Quinazolines and 1,4-Benzodiazepines. *Heterocycles* **1989**, *29*, 1477−1487.
(28) Fryer, R. I.; Pinto, J. C.; Upasani, R. B. Studies Related to Alkylations of Enolate Anions of 1,4-Benzodiazepinones. *J. Heterocyclic Chem.* **1993**, *30*, 945−951.
(29) Walser, A.; Flynn, T.; Fryer, R. I. Quinazolines and 1,4-Benzodiazepines. Lxxxv (I). Sintheses of 3-Substituted Imidazo-[1,5-a][1,4]benzodiazepines. *J. Heterocyclic Chem.* **1978**, *15*, 577−583.
(30) Petcher, T. J.; Widmer, A.; Maetzel, U.; Zeugner, H. Structures of Tifluadom [5-(2-fluorophenyl)-1-methyl-2-(3-thenoyl-aminomethyl)-2,3-dihydro-1H- 1,4-benzodiazepine]Hydrochloride, $C_{22}H_{21}FN_3OS^+ \cdot Cl^-$, and of (+)-Tifluadom *p*-Toluenesulphonate, $C_{22}H_{21}FN_3OS^+ \cdot C_7H_7O_3S^-$, and the Absolute Configuration of the Latter. *Acta Cryst.* **1985**, *C41*, 909−912.
(31) Kotzer, C. J.; Hay, D. W. P.; Dondio, M.; Giardina, G. A. M.; Petrillo, P.; Underwood, D. The Antitussive Activity of Delta Opioid Receptor Stimulation in Guinea Pigs. *J. Pharmacol. Exp. Ther.* **2000**, *292*, 803−809.
(32) Leighton, G. E.; Rodriguez, R. E.; Hill, R. G.; Hughes, J. kappa-Opioid Agonists Produce Antinociception after i.v. and icv but not Intrathecal Administration in the Rat. *Br. J. Pharmacol.* **1988**, *93*, 553−560.
(33) Pelissier, T.; Paeile, C.; Soto-Moyano, R.; Saavedra, H.; Hernandez, A. Analgesia Produced by Intrathecal Administration of the kappa Opioid Agonist, U-50, 488H, on Formalin-Evoked Cutaneous Pain in the Rat. *Eur J. Pharmacol.* **1990**, *190*, 287−293.
(34) Endoh, T.; Matsuura, H.; Tajima. A.; Izumimoto, N.; Tajima, C.; Suzuki, T.; Saitoh, A.; Suzuki, T.; Marita, M.; Tseng, L.; Nagase, H. Potent Antinociceptive Effects of TRK-820, a Novel kappa-Opioid Receptor Agonist. *Life Sci.* **1999**, *65*, 1685−1694.
(35) Stevens, C. W.; Yaksh, T. L. Dynorphin A and Related Peptides Administered Intrathecally in the Rat: A Search for Putative kappa Opiate Receptor Activity. *J. Pharmacol. Exp. Ther.* **1986**, *238*, 833−838.
(36) Colombo, P. J.; Martinez, J. L.; Bennet, E. L.; Rosenzweig, M. R. k-Opioid Receptor Activity Modulates Memory for Peck-Avoidance Training in the 2-Day-Old Chick. *Psycopharmacology* **1992**, *108*, 235−241.
(37) Ukai, M.; Itoh, J.; Kobayashi, T.; Shinkai, N.; Kameyama, T. Effects of the k-Opioid Dynorphin A-(1−13) on Learning and Memory in Mice. *Behav. Brain Res.* **1997**, *83*, 169−172.
(38) Hiramatsu, M.; Inoue, K.; Kameyama, T. Dynorphin A-(1−13) and (2−13) Improve β-Amyloid Peptide-Induced Amnesia in Mice. *Neuroreport* **2000**, *11*, 431−435.
(39) Ukai, M.; Shan-Wu, Y.; Kobayashi, T.; Kameyama, T. Systemic Administration of Dynorphin A-(1−13) Markedly Improves Cycloheximide-Induced Amnesia in Mice. *Eur. J. Pharmacol.* **1996**, *313*, 11−15.
(40) Ukai, M.; Shinkai, N.; Kameyama, T. k-Opioid Receptor Agonists Improve Pirenzepine-Induced Disturbance of Spontaneous Alternation Performance in the Mouse. *Eur. J. Pharmacol.* **1995**, *81*, 173−178.
(41) Hiramatsu, M.; Murasawa, H.; Nabeshima, T.; Kameyama, T. Effects of U-50,488H on Scopolamine-, Mecamylamine- and Dizocilpine-Induced Learning and Memory Impairment in Rats. *J. Pharmacol. Exp. Ther.* **1998**, *284*, 858−867.
(42) Henderson, R.; Baldwin, J.; Ceska, T. H.; Zemlin, F.; Beckmamn, E.; Downing, K. Model of the Structure of Bacteriorhodopsin Based on High-Resolution Electron Cryomicroscopy. *J. Mol. Biol.* **1990**, *213*, 899−919.
(43) Baldwin, J. M. The Probable Arrangement of the Helices in G Protein-Coupled Receptors. *The EMBO J.* **1993**, *12*, 1693−1703.
(44) Ballesteros, J. A.; Weinstein, H. Analysis and Refinement of Criteria for Predicting the Structure and Relative Orientations of Transmembranal Helical Domains. *Biophys. J.* **1992**, *62*, 107−109.
(45) Beukers, M. W.; Kristiansen, K.; Ijzerman, A. P.; Edvardsen, Ø. TinyGRAP Database: a Bioinformatics Tool to Mine G Protein-Coupled Receptor Mutant Data. *TiPS* **1999**, *20*, 475−477.
(46) Mansour, A.; Taylor, L. P.; Fine, J. L.; Thompson, R. C.; Hoversten, M. T.; Mosberg, H. I.; Watson, S. J.; Akil, H. Key Residues Defining the μ-Opioid Receptor Binding Pocket: a Site-Directed Mutagenesis Study. *J. Neurochem.* **1997**, *68*, 344−353.
(47) Xu, W.; Li, J.; Chen, C.; Huang, P.; Weinstein, H.; Javitch, J. A.; Shi, L.; De Riel, J. K.; Liu Chen, L. Y. Comparison of the Amino acid Residues in the Sixth Transmembrane Domains Accessible in the Binding-Site Crevices of mu, delta, and kappa Opioid Receptors. *Biochemistry* **2001**, *40*, 8018−8029.
(48) Metzger, T. G.; Paterlini, M. G.; Ferguson, D. M.; Portoghese, P. S. Investigation of the Selectivity of Oxymorphone- and Naltrexone-Derived Ligands via Site-Directed Mutagenesis of Opioid Receptors: Exploring the "Address" Recognition locus. *J. Med. Chem.* **2001**, *44*, 857−62.
(49) Sali, A.; Blundell, T. L. Comparative Protein Modeling by Satisfaction of Spatial Restraints. *J. Mol. Biol.* **1993**, *234*, 779−815.
(50) Thompson J. D.; Higgins D. G.; Gibson T. CLUSTAL W: Improving the Sensitivity of Progressive Multiple Sequence Alignment Through Sequence Weighting, Position-Specific Gap Penalties and Weight Matrix Choice. *J. Nucleic Acids Res.* **1994**, *22*, 4673−4680.
(51) Brooks, B. R.; Bruccoleri, R. E.; Olafson, B. D.; States, D. J.; Swaminathan, S.; Karplus, M. CHARMM: a Program for Macromolecular Energy Minimization and Dynamics Calculations. *J. Comput. Chem.* **1983**, *4*, 187−217.
(52) van Gunsteren, W. F.; Berendsen, J. C. Algorithms for Macromolecular Dynamics and Constraint Dynamics. *Mol. Phys.* **1977**, *34*, 1311−1327.
(53) Menziani, M. C.; De Benedetti, P. G.; Gago, F.; Richards, W. G. The Binding of Benzensulphonamides to Carbonic Anhidrase Enzyme. A Molecular Mechanics Study and Quantitative Structure−Activity Relationships. *J. Med. Chem.* **1989**, *32*, 951−956.
(54) Scheideler, M. A.; Zukin, R. S. Reconstitution of Solubilized Delta-Opiate Receptor Binding Sites in Lipid Vesicles. *J. Biol. Chem.* **1990**, *265*, 15176−15182.
(55) Baron, B. M.; Siegel, B. W.; Slone, A. L.; Harrison, B. L.; Palfreyman, M. G.; Hurt, S. D. [^{3}H]5,7-Dichlorokynurenic Acid, a Novel Radioligand Labels NMDA Receptor-Associated Glycine Binding Sites. *Eur. J. Pharmacol.* **1991**, *206*, 149−154.
(56) Cheng, Y. C.; Prusoff, W. H. Relationship Between the Inhibition Constant (K_i) and the Concentration of Inhibitor Which Causes 50 Per Cent Inhibition (I_{50}) of an Enzymatic Reaction. *Biochem. Pharmacol.* **1973**, *22*, 3099−3108.
(57) O'Callaghan, J. P.; Holtzman, S. G. Quantification of the Antinociceptive Activity of Narcotic Antagonists by a Modified Hot-Plate Procedure. *J. Pharmacol. Exp. Ther.* **1975**, *192*, 497−505.
(58) Jarvik, M. E.; Kopp, R. An Improved One-Trial Passive Avoidance Learning Situation. *Psychol. Rep.* **1967**, *21*, 221−224.
(59) Haley, T. J.; McCormick, W. G. Pharmacological Effects Produced by Intracerebral Injection of Drugs in the Conscious Mouse. *Br. J. Pharmacol. Chemother.* **1957**, *12*, 12−15.

JM0307640